

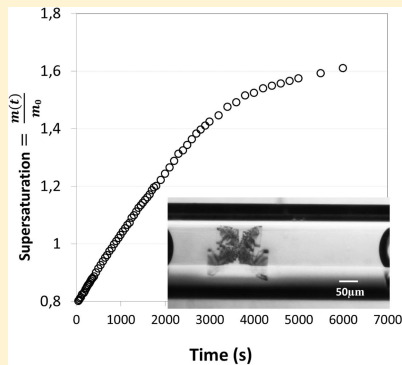
## Metastability Limit for the Nucleation of NaCl Crystals in Confinement

Julie Desarnaud,<sup>†</sup> Hannelore Derluyn,<sup>‡,§</sup> Jan Carmeliet,<sup>‡</sup> Daniel Bonn,<sup>†</sup> and Noushine Shahidzadeh\*,<sup>†</sup>

<sup>†</sup>Van der Waals-Zeeman Institute, Institute of Physics, University of Amsterdam, Science Park 904, 1098 XH Amsterdam, The Netherlands

<sup>‡</sup>ETH, Institut für Technologie in der Architektur, HIL E 46.3, Wolfgang-Pauli-Strasse 15, 8093 Zürich Hönggerberg, Switzerland

**ABSTRACT:** We study the spontaneous nucleation and growth of sodium chloride crystals induced by controlled evaporation in confined geometries (microcapillaries) spanning several orders of magnitude in volume. In all experiments, the nucleation happens reproducibly at a very high supersaturation  $S \sim 1.6$  and is independent of the size, shape, and surface properties of the microcapillary. We show from classical nucleation theory that this is expected:  $S \sim 1.6$  corresponds to the point where nucleation first becomes observable on experimental time scales. A consequence of the high supersaturations reached at the onset of nucleation is the very rapid growth of a single skeletal (Hopper) crystal. Experiments on porous media also reveal the formation of Hopper crystals in the entrapped liquid pockets in the porous network and consequently underline the fact that sodium chloride can easily reach high supersaturations, in spite of what is commonly assumed for this salt.



### SECTION: Surfaces, Interfaces, Porous Materials, and Catalysis

Sodium chloride is the most abundant salt on earth, and its crystallization is very important in many applications. Degradation and desertification of soils due to sodium chloride is a major physiological threat to ecosystems.<sup>1–3</sup> Moreover, its crystallization in confined conditions is known to be not only one of the major causes of physical weathering and disintegration of rocks, stones, and building materials,<sup>4–10</sup> but also constitutes a problem for oil well productivity and CO<sub>2</sub> storage due to increased impermeability of deep soil layers and rocks.<sup>11,12</sup> On the other hand, sea salt aerosols are one of the most abundant primary inorganic aerosols, and their kinetics of deliquescence/crystallization provide important insights to the alteration of the particle aerodynamic properties and their cloud-droplet nucleation efficiency.<sup>13</sup> For most if not all of the above-mentioned applications, the precise conditions under which NaCl crystals nucleate and grow from solution are very important but largely unknown.

Although recent simulations give us some more insight into the atomistic pathways of the nucleation of NaCl crystals,<sup>14–17</sup> the current consensus appears to be that no high supersaturations can be reached for this salt, and that the pore size has a profound influence on the concentration at which the nucleation is first observed,<sup>4,18–22</sup> in spite of the fact that typical pore sizes are orders of magnitude larger than the size of a critical nucleus.

Here, we report experiments on the primary nucleation and growth of sodium chloride crystals by controlled evaporation for different degrees of confinement in microcapillaries in which the salt solution is trapped by capillary forces. We use confined geometries consisting of glass microcapillaries of different sizes (from 20 to 2000  $\mu\text{m}$ ) with different surface

chemistries: hydrophobic (silanized) and hydrophilic (cleaned).<sup>23</sup> The geometry of the microcapillaries is also changed; besides cylindrical, we also use rectangular shapes, since, in real porous media, liquid can be trapped within corners of the porous network.<sup>23–26</sup> We study situations with slow evaporation (and, consequently, no large salt concentration gradients) by choosing the initial concentration in such a way that the surface tension and the contact angle of the salt solution were high enough to avoid the formation of wetting films.

We start out with aqueous solutions of known initial concentration  $m_i = 4.9 \text{ mol}\cdot\text{kg}^{-1}$  of NaCl (Sigma-Aldrich purity >99.9%) in Millipore water; the saturation concentration being  $m_0 = 6.15 \text{ mol}\cdot\text{kg}^{-1}$ ; the relative supersaturation  $S$  is then defined as  $m/m_0$ . The crystallization is induced by evaporation under isothermal conditions ( $T = 21 \pm 1^\circ\text{C}$ ): a known volume  $V_0$  (ranging from  $10^{-3}$  to 5  $\mu\text{L}$ ) of the solution is introduced into the capillary and placed into a miniature climatic chamber under a microscope. By fixing the relative humidity of the ambient air in the climatic chamber,<sup>6</sup> the evaporation rate of the solution is controlled. The volume change during the evaporation of the solutions inside the microcapillaries is subsequently followed by recording the displacement of the two menisci while simultaneously visualizing the onset of crystal growth in the solution directly with an optical microscope coupled to a CCD camera. The nucleation and

Received: January 15, 2014

Accepted: February 14, 2014

growth is observed to happen in the bulk of the solution, far from the walls and the interface.

Figure 1 shows the supersaturation at the onset of spontaneous crystal growth for different sizes, shapes, and surface chemistry of the capillaries and for different evaporation rates.

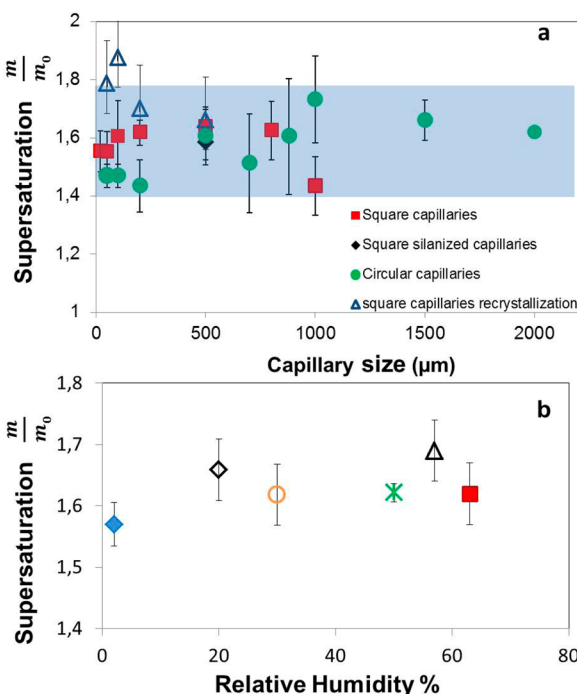


**Figure 1.** Supersaturation ( $S = m/m_0$ ) of NaCl solutions reached by evaporation at the onset of nucleation and growth ( $m$  and  $m_0$  are molalities  $\text{mol}\cdot\text{kg}^{-1}$  at the onset of crystallization and at equilibrium respectively): (a) data for microcapillaries of different sizes, geometries (square and circular), and wetting properties (cleaned and silanized) at  $\text{RH} \sim 52 \pm 2\%$ ; (b) data at different relative humidities for square microcapillary  $200 \mu\text{m}$ . Each point is an average of more than eight experiments; the error bar indicates the spread in the observed values.

From more than 100 experiments, a limit of supersolubility of  $S \sim 1.6 \pm 0.2$  is found. This is very high compared to the limit of metastability reported in the literature for sodium chloride in cooling experiments,  $S \sim 1.03$ .<sup>27–29</sup> In the latter experiments, clear saturated solutions obtained from a solution in contact with crystals were used for the cooling experiments. However, the fact that the solution is clear does not automatically imply that the saturated solution is completely devoid of tiny microcrystallites, which can greatly facilitate the formation of macroscopic ones.<sup>6,23</sup>

To assess a possible effect of impurities on the concentration for which nucleation is first observed, recrystallization experiments were conducted by performing repeated cycles of complete deliquescence (dissolution by water vapor) of the salt crystals followed by drying, a procedure that is known to efficiently expel impurities.<sup>6,30</sup> These results show again that the concentration reached at the onset of nucleation and crystal growth is not affected to within the experimental uncertainty (Figure 1a).

One difference between evaporation and cooling experiments is that, when the ion transport in the liquid phase is slower than the evaporation rate, there may be concentration gradients in the salt solution. This leads to a higher concentration of ions

close to the meniscus, where the evaporation takes place. To see whether our supersaturation is well-defined in terms of the NaCl concentration, we determine the Peclet number ( $\text{Pe}$ ), which is a measure of the heterogeneity of the ion distribution.  $\text{Pe}$  is defined as the ratio between the convective and the diffusive transport of ions in the solution and can be calculated from the (time-dependent) NaCl diffusion coefficient and the characteristic time of the displacement of the meniscus:<sup>24</sup>

$$\text{Pe} \approx t_{\text{diff}}/t_s \quad (1)$$

which in turn are given by  $t_{\text{diff}} \approx z_0^2/D_{\text{NaCl}}(t)$  and  $t_s \approx z_0/(dz/dt)$  with  $z_0$  the initial meniscus position,  $z$  the position at time  $t$ , and  $D_{\text{NaCl}}(t)$  the diffusion coefficient at time  $t$ , which depends on the concentration and viscosity of the solution.<sup>31</sup>

We find that  $\text{Pe}$  is of the order of unity at first, but reaches values on the order of  $10^{-2}$  to  $10^{-3}$  at the onset of nucleation. The latter underlines a homogeneous distribution of ions in the solution and is mainly due to the fact that the evaporation slows down, as shown in Figure 2.

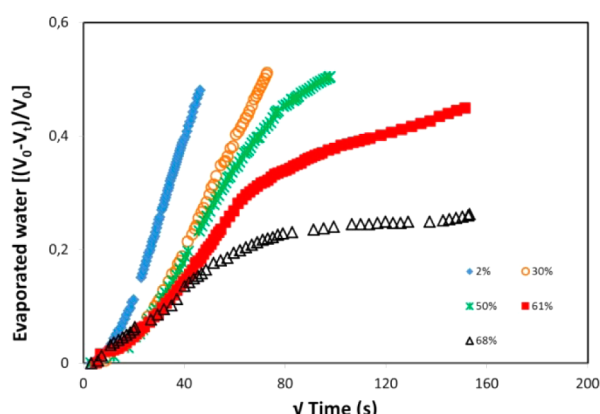


**Figure 2.** (a) Normalized evaporated water volume as a function of  $\sqrt{\text{time}}$  at different relative humidities until spontaneous crystal growth is observed ( $m_i = 4.9 \text{ mol}\cdot\text{kg}^{-1}$ ,  $d = 200 \mu\text{m}$  square capillaries).

When the evaporation rate  $e$  is limited by diffusive vapor transport through the gas phase, it is given by<sup>24,32</sup>

$$e \approx \rho_g D \frac{(c_i - c_\infty)}{\delta} \quad (2)$$

with  $\rho_g$  the vapor density,  $D$  the diffusion coefficient of water vapor through the gas,  $c_\infty$  the controlled water vapor concentration of the climatic chamber and  $c_i$  the water vapor concentration just above the menisci;  $\delta$  is the characteristic distance over which diffusion takes place. The drying rate is consequently controlled by  $\delta$  and  $(c_i - c_\infty)$ ; the evaporation  $(c_i - c_\infty)$  decreases because the saturated vapor concentration decreases when the salt solution becomes more concentrated ( $c_i/c_{\text{pure water}} = 1 - 0.24 S^{33}$ ); on the other hand,  $\delta$  is roughly the distance between the meniscus and the outlet of the capillary, which increases; both effects then lead to a decrease in evaporation rate with time, and, consequently, a simple diffusive  $\sqrt{t}$  scaling is not expected.<sup>32,34</sup>

The necessary time to reach the concentration at which the spontaneous nucleation and growth is observed depends on the relative humidity and varies over more than an order of magnitude. However, it is interesting to note that, independently of the time necessary to reach it, the crystallization is only observed when the supersaturation of 1.6 is achieved. As a

consequence, for humidities higher than 61%, corresponding to the equilibrium water vapor concentration above a solution close to our limit of supersolubility ( $S \sim 1.6$ ), the evaporation rate goes to zero as soon as  $c_i = c_\infty$  (Figure 2, black symbols). Here, in spite of the fact that the solution is supersaturated, nucleation is not observed because the supersaturation 1.6 is not reached. The metastable supersaturated solution can remain for days without any spontaneous crystallization until a perturbation is introduced to the system (i.e., rapid decrease of the temperature or water vapor concentration in the air) triggers the nucleation. This series of experiments independently provides another value for the onset of nucleation:  $S = 1.60 \pm 0.07$  (Figure 1b), in agreement with the findings above.

It is worth noting here that the time delay between the actual nucleation and our first observation of the crystal is given by its growth rate, which is typically on the order of a few ( $\sim 5$ )  $\mu\text{m/s}$  for the cubic NaCl crystal.<sup>6</sup> This means that within a few seconds of its formation, the crystal is consequently observable. This results in an error on the supersaturation that is negligible, since the evaporation takes place over several hours. Moreover, any crystallization in the solution would change the equilibrium water vapor pressure above the solution and consequently the evaporation rate; we only observe such a change when we also observe the crystal.

Since the nucleation appears to be homogeneous, Classical Nucleation Theory (CNT) can be used to predict the rate of crystal nucleation for sodium chloride as a function of the supersaturation. According to CNT, the rate of nucleation per unit volume can be calculated as the product of an exponential factor and a kinetic prefactor:<sup>35,36</sup>

$$J = \kappa \exp\left(-\frac{\Delta G^*}{kT}\right) \quad (3)$$

In the exponential factor,  $\Delta G^*$  is the free energy cost of creating a critical nucleus and  $kT$  the thermal energy. The total Gibbs free-energy cost to form a spherical crystallite has a bulk and a surface term and can be expressed as

$$\Delta G = \frac{4}{3} \pi R^3 \rho_s \Delta \mu + 4\pi R^2 \gamma \quad (4)$$

with  $\rho_s$  being the number density of solid,  $\Delta \mu$  the difference in chemical potential of the solid and liquid, and  $\gamma$  is the interfacial tension of the NaCl crystal with the solution ( $\gamma_{\text{lc}} \sim 0.08 \text{ N m}^{-1}$ ).<sup>35,37</sup> Here, the difference in chemical potential of the solid and liquid can be written in terms of the mean ionic activity of the solute,  $a_{\pm}$ ,<sup>4,27</sup> as

$$\frac{\mu_1 - \mu_c}{RT} = \nu \ln\left(\frac{a_{\pm}}{a_{0\pm}}\right) = \nu \ln\left(\frac{\gamma_{\pm} m}{\gamma_{0\pm} m_0}\right) \quad (5)$$

where  $m$  and  $m_0$  are the molalities at crystallization and equilibrium ( $\text{mol kg}^{-1}$ ),  $\gamma_{\pm}$  is the corresponding mean ionic activity coefficient, and  $\nu$  is the sum of ions (2 for NaCl).

The energy of the critical nucleus  $\Delta G^*$  is then

$$\Delta G^* = \frac{4\pi}{3} \gamma R_c^{*2} \quad \text{with} \quad R_c^* = \frac{2\gamma}{\nu k T \rho_s \ln\left(\frac{\gamma_{\pm} m}{\gamma_{0\pm} m_0}\right)} \quad (6)$$

The kinetic prefactor  $\kappa$ , which relates the efficiency with which collisions between supernatant ions and the crystal interface produce crystal growth, is determined from  $\kappa = \rho j Z$ , where  $\rho$  is the number density of molecules in the liquid phase,

$Z$  is the Zeldovich factor:  $Z \approx 1/(n^*)^{2/3}$  with  $n^*$  the excess number of molecules in the critical nucleus, and  $j$  is the rate at which molecules attach to the nucleus causing its growth.  $j$  is approximated as  $j \sim \rho D R^*$  with  $D$  being the diffusion constant of the molecules and  $R_c^*$  the radius of the critical nucleus.<sup>36</sup>

The rate of nucleation  $J (\text{m}^{-3} \text{s}^{-1})$  is plotted as a function of the supersaturation in Figure 3. It follows that, below  $S \sim 1.6$

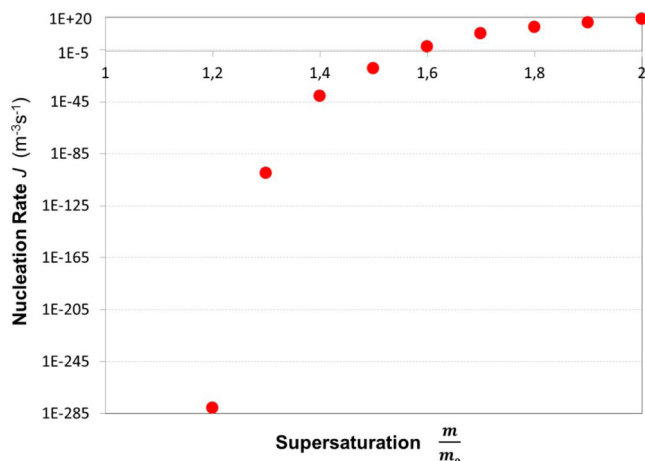
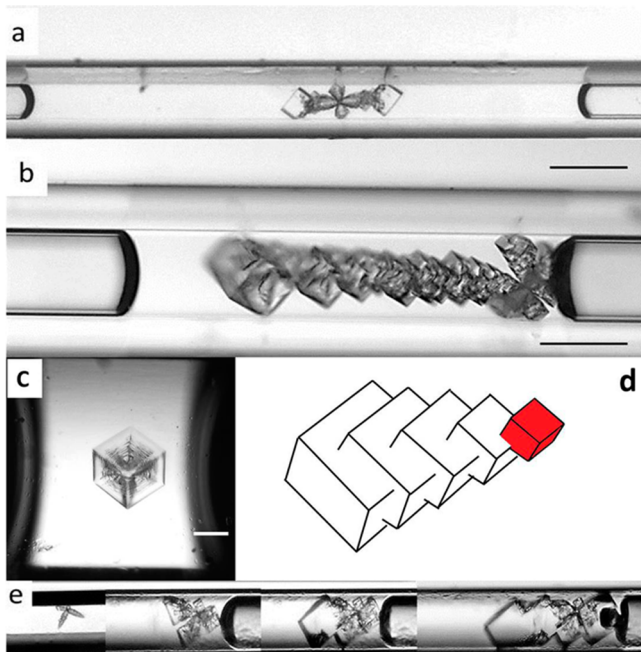


Figure 3. Nucleation rate  $J (\text{m}^{-3} \text{s}^{-1})$  as a function of supersaturation  $S = m/m_0$  of the solution.

the nucleation rate is extremely small and, conversely, very large above it. At  $S \sim 1.6$  the rate of the nucleation of sodium chloride is found to be  $0.004 \text{ m}^{-3} \text{ s}^{-1}$ , which roughly corresponds to one nucleus in a typical volume considered here within our experimental time window (typically 5000 s). Moreover, the variation of the experimental parameters here (volume  $V$ , relative humidity, etc.) does not significantly change the value of  $S \sim 1.6$  for which the nucleation becomes observable. Simply said, the nucleation rate depends so steeply on the supersaturation that all other parameters are irrelevant, in excellent agreement with all our observations.

Very recent simulations on NaCl solutions show surprisingly that already at a relatively low supersaturation, nucleation can be observed in smaller system than ours on the time scale of a simulation<sup>16,17</sup> that is shorter than our experimental time. This discrepancy could be an artifact of the model potentials used in the simulations or due to the different choice of parameters (attempt frequency, dielectric constant, chemical potential difference and surface tension) compare to the experimental ones. For example, the solubility of NaCl is underestimated in the simulations compare to the real value; this seems an appealing problem for further investigations.

Another very interesting observation is that at the onset of crystallization a single nucleus is observed to be growing very rapidly and with a peculiar shape: a Hopper (skeletal) crystal (Figure 4). The growth of the Hopper crystals in these experiments happens at a speed that can be up to 10 times that of the growth of a regular cubic crystal under the same conditions.<sup>6</sup> The rapid growth of the Hopper crystal is due to the high supersaturations for which secondary nucleation may occur at the corners of the growing primary nuclei, due to the disparity of growth rates between the crystal edges and the crystal faces.<sup>38–40</sup> In our experiment, this shows up as the rapid formation of a chain-like structure of crystals (Figure 4). For the formation of the Hopper crystal, the supersaturation has to be significantly above the saturation concentration, since it is



**Figure 4.** Spontaneous growth of Hopper crystals at supersaturation  $S \sim 1.6$ , in capillaries: (a)  $50 \mu\text{m}$ , (b)  $100 \mu\text{m}$ , (c)  $1000 \mu\text{m}$ , and (d) schematic presentation of the growth from one of the edges of the crystal (in red). (e) Evolution of the growth of a Hopper crystal in the first 10 min (scale =  $100 \mu\text{m}$ ).

well established that their formation requires a two-dimensional nucleation growth (Kossel–Stranski–Volmer) mechanism.<sup>27,40,41</sup> This mechanism involves the creation of two-dimensional ‘islands’ of molecules that subsequently spread outward, and the supersaturation needs to be high to ensure the stability of these adatoms that form on a flat surface.<sup>41</sup>

However, since the nucleation rate depends very steeply on the concentration, such a rapid growth of the critical nucleus will lead to a very rapid decrease of the local supersaturation and consequently favors the formation of only a single skeletal crystal. On the other hand, it is also shown that in a small system, the very rapid decrease of the local supersaturation during the growth of the critical nucleus favors the formation of one single nucleus.<sup>42</sup>

As the capillaries are often used as a model system for crystallization in pores, it is likely that such fast growth dynamics may provoke damage in porous materials; indeed, the crystallization pressure that is responsible for the damage is known to depend strongly on the supersaturations reached,<sup>43</sup> the size of the crystal,<sup>44</sup> and the speed of growth.<sup>45</sup> The range of capillary sizes used here in fact interpolates between evaporation in bulk for the largest capillaries and evaporation in pores representative of typical porous media such as natural stones and soils.<sup>6,46,47</sup>

To see whether our conclusions from the capillaries also apply to real porous media, we compare the crystal morphologies in microcapillaries at the late stages of drying with the NaCl crystals formed in experiments on porous sandstone (Mešné/Prague sandstone with average pore diameter  $d \sim 30 \mu\text{m}$  and porosity  $\sim 29\%$ ).<sup>5</sup>) The crystallization of NaCl in stones can lead to damage,<sup>7</sup> but the mechanisms are still under debate. A thermodynamic calculation<sup>4</sup> predicts that for equal supersaturations, sodium chloride can be more destructive than other salts (e.g., sodium sulfate), although

experimentally the opposite is observed. Consequently, if the damage potential of difference salts is to be compared, the question rather is whether a sufficient degree of supersaturation can be easily achieved with sodium chloride in porous media.

To be able to compare the capillaries and natural sandstone, the formation of entrapped liquid pockets in the porous network was facilitated by treating the surface of the stone with a water repellent product (silanes). The treatment slows down the evaporation, prevents salt from crystallizing at the exterior of the stone, and facilitates the formation of liquid pockets. After saturation of the stone with the initial salt solution ( $m_i = 4.9 \text{ mol}\cdot\text{kg}^{-1}$ ), the latter is dried under the same environmental conditions as the capillaries. Subsequently, the sample is fractured, and the salt crystal morphology inside the stone is investigated by scanning electron microscopy (SEM).

Figure 5 shows the remarkable similarities between the crystal structures formed in the stone after complete drying and

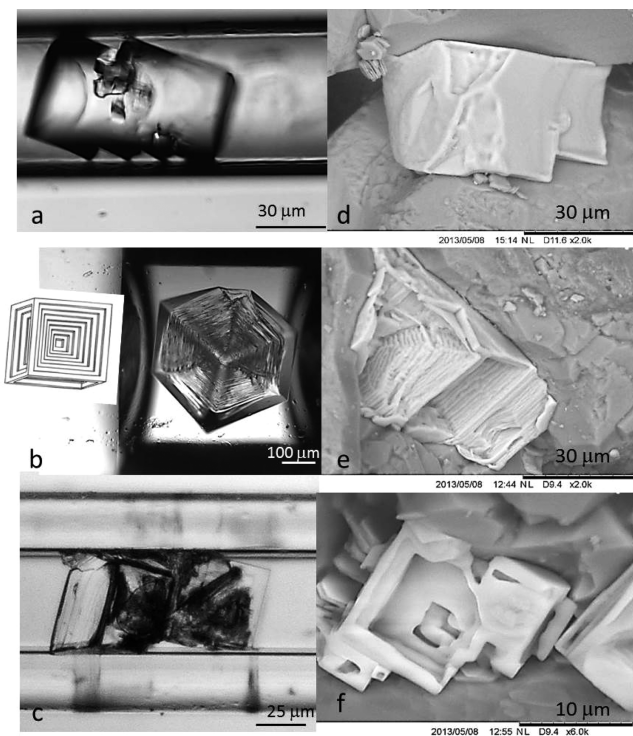


**Figure 5.** Comparison between NaCl crystals formed in capillaries after reaching our limit of supersolubility  $S \sim 1.6$  (a–c) and those obtained in the sandstone (d–f). All the experiments are done at ( $T = 21^\circ\text{C}$ , RH  $\sim 50\%$ ).

in the capillaries: in the stone, Hopper crystals have also formed. Observations on several samples show that these crystals shape are plentiful in some regions of the stone, and almost absent from others, suggesting that very concentrated residual fluid pockets had formed during the evaporation. Both these observations indicate for the first time that the liquid pockets in the stone behave similarly to the microcapillaries where high supersaturations were reached before crystallization sets in. This supersaturation seems to be sufficient to provoke weathering. In fact, at  $S = 1.6$ , the crystallization pressure<sup>4</sup> is about  $\Delta P \sim 160 \text{ MPa}$ . If we assume that only 15% of local volume fraction is filled with the salt, the related effective stress<sup>48,49</sup> in the sandstone will be  $\sigma^* \sim 1.65 \text{ MPa}$ , which is

higher than the tensile strength of the Mešne sandstone (0.9 MPa).

In sum, we have demonstrated by controlled evaporation experiments of sodium chloride solutions that the supersaturation achieved at the onset of spontaneous primary nucleation and growth is around 1.6 and remains independent of the size, shape, and surface properties of the microcapillary. These results are consistent with expectations from classical nucleation theory. The supersolubility limit obtained here clearly shows that, contrary to what is commonly assumed for this salt,<sup>18,21,28,29,50</sup> high concentrations can be reached before spontaneous crystal growth. This in turn leads to the formation of a Hopper crystal, which we also detected in analogous experiments conducted on real sandstone. Our findings therefore have far-reaching implications for the widespread consequences of salt crystallization,<sup>1–12,51</sup> since the salt weathering of rocks, stones, and monuments is related to the crystallization pressure, which is directly dictated by the supersaturation and the importance of which is expected to increase in the future due to global climate change.<sup>52</sup>

## AUTHOR INFORMATION

### Corresponding Author

\*E-mail: n.shahidzadeh@uva.nl.

### Present Address

<sup>§</sup>H.D.: Ghent University, Department of Geology and Soil Science - UGCT, Krijgslaan 281 S8, 9000 Gent, Belgium.

### Notes

The authors declare no competing financial interest.

## ACKNOWLEDGMENTS

This work is funded by Stichting Fundamenteel Onderzoek der Materie (FOM), which is part of The Netherlands Organisation for scientific research (NWO). H.D. is a postdoctoral fellow of the Research Foundation - Flanders (FWO) and acknowledges its support.

## REFERENCES

- (1) Rengasamy, P.; Olsson, K. A. Sodicity and Soil Structure. *Aust. J. Soil Res.* **1991**, *29*, 935–952.
- (2) Wong, V. N.; Dalal, R. C.; Greene, R. S. Salinity and Sodicity Effects on Respiration and Biomass of Soil. *Biol. Fert. Soils* **2008**, *44*, 943–953.
- (3) Cook, R. U.; Smalley, I. J. Salt Weathering in Deserts. *Nature* **1968**, *220*, 1226–1227.
- (4) Steiger, M. Growth in Porous Materials – I: The Crystallization Pressure of Large Crystals. *J. Cryst. Growth* **2005**, *282*, 455–469.
- (5) Shahidzadeh-Bonn, N.; Desarnaud, J.; Bertrand, F.; Chateau, X.; Bonn, D. Damage in Porous Media Due to Salt Crystallization. *Phys. Rev. E* **2010**, *81*, 066110-1–6.
- (6) Shahidzadeh, N.; Desarnaud, J. Damage in Porous Media: Role of the Kinetics of Salt (Re)Crystallization. *Eur. Phys. J. Appl. Phys.* **2012**, *60*, 24205-1–7.
- (7) Lubelli, B.; van Hess, R. P. J.; Huinink, H. P.; Groot, C. J. W. P. Irreversible Dilation of NaCl Contaminated Lime-Cement Mortar due to Crystallization Cycles. *Cem. Concr. Res.* **2006**, *36*, 678–687.
- (8) Espinosa-Marzal, R.; Scherer, G. W. Impact of In-Pore Salt Crystallization on Transport Properties. *Environ. Earth Sci.* **2013**, *69*, 2657–2669.
- (9) Schiro, M.; Ruiz-Agudo, E.; Rodriguez-Navarro, C. Damage Mechanisms of Porous Materials due to In-Pore Salt Crystallization. *Phys. Rev. Lett.* **2012**, *109*, 265503-1–5.
- (10) Veran-Tissoires, S.; Marcoux, M.; Prat, M. Discrete Salt Crystallization at the Surface of a Porous Medium. *Phys. Rev. Lett.* **2012**, *108*, 054502-1–4.
- (11) Muller, N.; Qi, R.; Mackie, E.; Pruess, K.; Blunt, M. J. CO<sub>2</sub> Injection Impairment due to Halite Precipitation. *Energy Proc.* **2009**, *1*, 3507–3514.
- (12) Peysson, Y. Permeability Alteration Induced by Drying of Brines in Porous Media. *Eur. Phys. J. Appl. Phys.* **2012**, *60*, 24206-1–12.
- (13) Li, X.; Dhrubajyoti, D.; Hyo-Jin, E.; Hye Kyeong, K.; Chul-Un, R. Deliquescence and Efflorescence Behavior of Individual NaCl and KCl Mixture Aerosol Particles. *Atmos. Environ.* **2014**, *82*, 36–43.
- (14) Zahn, D. Atomistic Mechanism of NaCl Nucleation from an Aqueous Solution. *Phys. Rev. Lett.* **2004**, *92*, 040801-1–4.
- (15) Mucha, M.; Jungwirth, P. Salt Crystallization from an Evaporating Aqueous Solution by Molecular Dynamics Simulations. *J. Phys. Chem. B* **2003**, *107*, 8271–8274.
- (16) Chakraborty, D.; Patey, G. N. How Crystals Nucleate and Grow in Aqueous NaCl Solution. *J. Phys. Chem. Lett.* **2013**, *4*, 573–578.
- (17) Chakraborty, D.; Patey, G. N. Evidence that Crystal Nucleation in Aqueous NaCl Solution Occurs by the Two Step Mechanism. *Chem. Phys. Lett.* **2013**, *587*, 25–29.
- (18) Emmanuel, S.; Berkowitz, B. Effect of Pores Size Controlled Solubility on Reactive Transport in Heterogeneous Rock. *Geophys. Res. Lett.* **2010**, *34*, L06404-1–5.
- (19) Putnis, A.; Mauthe, G. The Effect of Pore Size on Cementation in Porous Rocks. *Geofluids* **2001**, *1*, 37–41.
- (20) Flatt, R. J. Salt Damage in Porous Materials: How High Supersaturations are Generated. *J. Cryst. Growth* **2002**, *242*, 435–454.
- (21) Bouzid, M.; Mercury, L.; Lassin, A.; Matray, J. M. Salt Precipitation and Trapped Liquid Cavitation in Micrometric Capillary Tubes. *J. Colloid Interface Sci.* **2011**, *360*, 768–776.
- (22) Sekine, K.; Okamoto, A.; Hayashi, K. In Situ Observation of the Crystallization Pressure Induced by Halite Crystal Growth in a Microfluidic Channel. *Am. Mineral.* **2011**, *96*, 1012–1019.
- (23) Shahidzadeh-Bonn, N.; Rafai, S.; Bonn, D.; Wegdam, G. Salt Crystallization during Evaporation: Impact of Interfacial Properties. *Langmuir* **2008**, *24*, 8599–8605.
- (24) Camassel, B.; Sghaier, N.; Prat, M.; Nasrallah, S. B. Evaporation in a Capillary Tube of Square Cross-Section: Application to Ion Transport. *Chem. Eng. Sci.* **2005**, *60*, 815–826.
- (25) Wong, H.; Morris, S.; Radke, C. J. Three Dimensional Menisci in Polygonal Capillaries. *J. Colloid Interface Sci.* **1992**, *148*, 317–336.
- (26) Chauvet, F.; Duru, P.; Geoffroy, S.; Prat, M. The Three Periods of Drying of a Single Square Capillary Tube. *Phys. Rev. Lett.* **2009**, *18* (124502), 1–4.
- (27) Mullin, J. W. *Crystallization*, 4<sup>th</sup> ed.; Butterworths-Heinemann: Oxford, 2001.
- (28) Chianese, A.; Cave, D. I.; Matzarotta, S. Solubility and Metastable Zone Width of Sodium Chloride in Water–Diethylene Glycol Mixtures. *J. Chem. Eng. Data* **1986**, *31*, 329–332.
- (29) Ginde, R. G.; Meyrson, A. S. Effect of Impurities on Cluster Growth and Nucleation. *J. Cryst. Growth* **1993**, *126*, 216–222.
- (30) Desarnaud, J.; Shahidzadeh-Bonn, N. Salt Crystal Purification by Deliquescence/Crystallization Cycling. *Europhys. Lett.* **2011**, *95* (48002), 1–6.
- (31) Kestin, J.; Khalifa, E.; Correia, R. J. Tables of the Dynamics and Kinematic Viscosity of Aqueous NaCl Solutions in the Temperature Range 20–150°C and the Pressure Range 0.1–35 MPa. *J. Phys. Chem. Ref. Data* **1981**, *10*, 71–87.
- (32) Bird, R. B.; Stewart, W. E.; Lightfoot, E. N. *Transport Phenomena*; Wiley: New York, 1960.
- (33) Robinson, R. A. The Vapour Pressures of Solutions of Potassium Chloride and Sodium Chloride. *Trans. R. Soc. New Zealand* **1945**, *75*, 203–217.
- (34) Holyst, R.; Litniewski, M.; Jakubczyk, D.; Kolwas, K.; Kolwas, M.; Kowalski, K.; Migacz, S.; Palesa, S.; Zientara, M. Evaporation of Freely Suspended Single Droplets: Experimental, Theoretical and Computational Simulations. *Rep. Prog. Phys.* **2013**, *76*, 034601-1–19.

- (35) Valeriani, C.; Sanz, E.; Frenkel, D. Rate of Homogeneous Nucleation in Molten NaCl. *J. Chem. Phys.* **2005**, *122*, 194501-1–6.
- (36) Sear, R. Nucleation: Theory and Applications to Protein Solutions and Colloidal Suspensions. *J. Phys.: Condens. Matter* **2007**, *19*, 033101-1–28.
- (37) Han-Soo, N.; Stephen, A.; Mayerson, A. S. Cluster Formation in Highly Supersaturated Solution Droplets. *J. Cryst. Growth.* **1994**, *139*, 104–112.
- (38) Kuroda, T.; Irisawa, T.; Okawa, A. Growth of a Polyhedral Crystal from Solution and Its Morphological Stability. *J. Cryst. Growth.* **1972**, *42*, 41–46.
- (39) Zhu, J. P.; Yu, S. H.; He, Z. B.; Jiang, J.; Chen, K.; Zhou, X. Y. Complex PbTe Hopper (Skeletal) Crystals with High Hierarchy. *Chem. Commun.* **2005**, 5802–5804.
- (40) Sunagawa, I. Growth and Morphology of Crystals. *Forma* **1999**, *14*, 147–166.
- (41) De Yoreo, J. J.; Vekilov, P. Principles of Crystal Nucleation and Growth. *Mineral. Soc. Am.* **2003**, *54*, 57–93.
- (42) Grossier, R.; Veesler, S. Reaching One Single and Stable Critical Cluster Through Finite-Sized Systems. *Cryst. Growth Des.* **2009**, *9*, 1017–1922.
- (43) Correns, C. W. Growth and Dissolution of Crystals Under Linear Pressure. *Discuss. Faraday Soc.* **1949**, *5*, 267–271.
- (44) Steiger, M. Crystal Growth in Porous Materials II: Influence of Crystal Size on the Crystallization Pressure. *J. Cryst. Growth.* **2005**, *282*, 470–481.
- (45) Chatterij, S. Aspects of Generation of Destructive Crystal Growth Pressure. *J. Cryst. Growth* **2005**, *277*, 566–577.
- (46) Choquette, P. W.; Pray, L. C. Geological Nomenclature and Classification of Porosity in Sedimentary Carbonates. *AAPG Bull.* **1970**, *54*, 207–250.
- (47) Rueldrich, J.; Seidel, M.; Rothert, E.; Siegesmund, S. Length Changes of Sandstone Caused by Salt Crystallization. In *Building Stone and Decay: From Diagnosis to Conservation*; Pfikryl, R., Smith, B. J., Eds.; Geological Society of London: Bath, U.K., 2007; Vol. 271, pp 199–209.
- (48) Espinosa-Marzial, R.; Hamilton, A.; McNall, M.; Whitaker, K.; Scherer, G. W. The Chemomechanics of Crystallization During Rewetting of Limestone Impregnated with Sodium Sulfate. *J. Mater. Res.* **2011**, *26*, 1472–1481.
- (49) Derluyn, H.; Mooneen, P.; Carmeliet, J. Deformation and Damage due to Drying Induced Salt Crystallization in Porous Limestone. *J. Mech. Phys. Solids* **2014**, *63*, 242–255.
- (50) Sghaier, N.; Prat, M.; Ben Nasrallah, S. On Ions Transport During Drying in a Porous Medium. *Trans. Porous Media* **2007**, *67*, 243–274.
- (51) Kiyohara, K.; Takushi Sugino, A.; Asaka, K. Electrolytes in Porous Electrodes: Effects of the Pore Size and the Dielectric Constant of the Medium. *J. Chem. Phys.* **2010**, *132*, 144705-1–12.
- (52) *Climate Change and World Heritage: Report on Predicting and Managing the Impacts of Climate Change on World Heritage and Strategy to Assist States Parties to Implement Appropriate Management Responses*; Augustin, C., Ed.; UNESCO World Heritage Centre: Paris, 2007.